Available online at www.sciencedirect.com

SCIENCE DIRECT®

Journal of Molecular Spectroscopy 226 (2004) 1–6

Journal of MOLECULAR SPECTROSCOPY

www.elsevier.com/locate/jms

Cavity ring-down spectroscopy of $H_2{}^{18}O$ in the range 16 570–17 120 cm^{-1} ☆

Mizuho Tanaka,[a] Maarten Sneep,[b] Wim Ubachs,[b] and Jonathan Tennyson[a,*]

[a] Department of Physics and Astronomy, University College London, London WC1E 6BT, UK
[b] Laser Centre, Department of Physics and Astronomy, Vrije Universiteit, De Boelelaan 1081, 1081 HV Amsterdam, The Netherlands

Received 19 November 2003; in revised form 1 March 2004
Available online 9 April 2004

Abstract

Cavity ring-down spectroscopy is used to record an absorption spectrum of $H_2{}^{18}O$ water vapor in the 16 570–17 120 cm^{-1} region. In the spectrum, 596 lines are identified as belonging to $H_2{}^{18}O$, of which 375 lines are assigned by comparing to newly calculated theoretical lines. The spectrum covers the entire 5ν polyad and two new vibrational band origins, (321) at 16775.381 cm^{-1} and (401) at 16854.991 cm^{-1} are determined.
© 2004 Elsevier Inc. All rights reserved.

1. Introduction

The absorption spectrum of water vapor is being comprehensively studied nowadays due to the high demand for accurate data for many aspects of science. Taking atmospheric science as an example, water vapor is the most important greenhouse gas and the major absorber of incoming sunlight. Besides the most abundant $H_2{}^{16}O$, its second most abundant isotopomer $H_2{}^{18}O$ also contributes significantly to the absorption of solar radiation. Knowing the precise line positions and strengths of water isotopomers would therefore increase the accuracy of atmospheric modeling of the Earth as a whole. Furthermore, the 5ν region studied here lies in a window used for remote sensing [1]. $H_2{}^{18}O$ has been much less extensively studied compared to $H_2{}^{16}O$ and there has been no previous work on this isotopomer in this region.

The first experiment on $H_2{}^{18}O$ at visible wavelengths was carried out in the early 1980s using the McMath Fourier transform spectrometer by Chevillard and coworkers at the National Solar Observatory (Kitt Peak, AZ). They recorded long-pathlength spectra with isotopically enriched $H_2{}^{18}O$ and $H_2{}^{17}O$ samples over a wide frequency range and a series of papers have analyzed these experimental results [2–12]. The data on $H_2{}^{18}O$ in the HITRAN2000 database [13] are limited, with the highest frequency listed for $H_2{}^{18}O$ being 13 900 cm^{-1} whereas for $H_2{}^{16}O$, the data extends to over 22 600 cm^{-1}. In addition, we found that this database appears to lack the entire 2ν polyad region of $H_2{}^{18}O$ which Toth has extensively analyzed [6].

A recent analysis of the $H_2{}^{18}O$ spectrum by Tanaka et al. [11] extended the frequency range analyzed up to 14 520 cm^{-1}, completely covering the $3\nu + \delta$ and 4ν polyads regions. In this study, pulsed cavity ring-down spectroscopy was used to record 16 570–17 120 cm^{-1} frequency range which covers the 5ν polyad region. Naus et al. [14] studied the same frequency region for natural abundance water. This work concentrated on $H_2{}^{16}O$ lines but also tentatively identified some transitions due to $H_2{}^{18}O$.

2. Experimental details

The experimental apparatus used in this experiment is the same as the one used in the earlier measurements on $H_2{}^{16}O$ [14]. Wavelength tunable laser pulses with a bandwidth of ~0.06 cm^{-1}, produced by a Nd:YAG

☆ Supplementary data for this article are available on ScienceDirect (www.sciencedirect.com) and as part of the Ohio State University Molecular Spectroscopy Archives (http://msa.lib.ohio-state.edu/jmsa_hp.htm).

* Corresponding author. Fax: +44-20-7679-7145.
E-mail address: j.tennyson@ucl.ac.uk (J. Tennyson).

0022-2852/$ - see front matter © 2004 Elsevier Inc. All rights reserved.
doi:10.1016/j.jms.2004.03.004

pumped dye laser system (Quanta Ray PDL-3) were used in a generic pulsed CRD experiment. The ring-down cell was 86.5 cm long and a single mirror set, with reflectivities varying between 99.97% near 16 500 cm^{-1} and 99.995% near 17 000 cm^{-1}, was used over the entire wavelength range. The radius of curvature of the mirrors is 1 m, and the stable cavity was aligned such that the statistics on the weighted residuals of a least squares fit were fully explained by contributions from Gaussian noise caused by the electronics and Poisson noise caused by the photon shot noise [15].

Before starting the measurements, the cell was heated to about 60 °C and flushed with dry nitrogen to remove as much of the natural water vapor from the cell as possible, without risk of damage to the mirrors. The liquid isotope enriched water—Euriso-top 96.5% atom ^{18}O, 0.6% atom ^{17}O, 2.9% atom ^{16}O—was injected into the cavity while flushing the opening with a continuous dry nitrogen flow. The cell was then closed and partly evacuated, and several hours were allowed for the pressure to stabilize. In order not to loose isotopically enriched water, part of the dry nitrogen was left in the cell. The temperature in the cell was measured and the partial water vapor density in the cell was calculated assuming saturation density. The partial water vapor pressure at the set temperature corresponds to 24 mbar. To avoid condensation on the mirrors, the mirror-mounts were gently heated.

Data points were taken at a step size of 0.008 cm^{-1} with averaging of five laser pulses at each laser frequency. The decay transients were detected using a photomultiplier tube, fed into a digital storage oscilloscope, and then transferred to a computer where a least squares fitting routine was used to estimate the decay rates. This fitting routine is the same as the one used in aligning the cavity. These decay rates contain both the water vapor absorption spectrum and a background signal caused by the losses of the empty cavity; this smooth background was subtracted from the spectrum before analyzing the resonance features. By recording an iodine spectrum simultaneously with the cavity ring-down spectrum a frequency calibration was obtained by comparing and interpolating the iodine spectrum against a reference atlas [16].

The spectra were searched by a computer program for possible locations of resonance features. A Voigt profile was then fitted to each of these candidate locations, yielding the central frequency, line width, and intensity. The entire spectrum was visually inspected to ensure that all fitted features were actual lines. Given the step size, the laser bandwidth and the width of the fitted lines, the one standard deviation error on the central frequency is estimated to be 0.01 cm^{-1}. The integrated line intensities, before correction associated with $H_2{}^{16}O$ contamination in the sample, were calculated using the fitted line parameters. Several error contributions can be distinguished in cavity ring-down spectroscopy: statistical effects, on the order of a few % in this experiment, a systematic underestimated absorption cross-section on narrow band absorbers [17] and saturation effects related to non-exponential decay in the ring-down transients of the strongest lines. An additional error that is specific for this experiment is the uncertainty in the isotopic content of the ring-down cell. An estimate of the isotope ratio of $H_2{}^{16}O$ and $H_2{}^{18}O$ is given below, but a few % uncertainty must be added to the error budget. The total error on the line intensities is estimated to be 15%. The complete list of lines containing both the center frequencies and loss-rates is available in the electric archive.

Despite our best effort to avoid contamination of the isotope enriched sample, several lines of $H_2{}^{16}O$ were visible in the measured spectrum. To weed out these $H_2{}^{16}O$ lines and identify which lines are $H_2{}^{18}O$ lines, we compared our new spectrum with the previously measured spectrum, by plotting both in a single graph and manually assign each line to either $H_2{}^{16}O$ or $H_2{}^{18}O$; see Fig. 1 for a short portion of both spectra. In Fig. 1, the vertical axes are given in terms of a cross-section per molecule. From the integrated intensity ratio of the $H_2{}^{16}O$ lines in both spectra, the isotope ratio in the spectra can be estimated. Using this approach yields a $H_2{}^{16}O$ contamination of about 10%. The integrated line intensities in the full spectrum are corrected for the isotope ratio in the cell.

The comparison between the measurements on the two isotopes clearly shows that the $H_2{}^{18}O$ lines are broader than the $H_2{}^{16}O$ lines, the difference being caused by the pressure conditions during the measurements. The width of the lines is ~0.13 cm^{-1} after fitting the spectra to a Voigt profile. This broadening beyond the laser linewidth of 0.06 cm^{-1} is a result of collision broadening. Doppler broadening and self-broadening at 24 mbar of water vapor yields a width of 0.09 cm^{-1}, the remainder of the broadening is attributed to nitrogen left behind in the cell during partial evacuation. The integrated intensities should be unaffected by the collisional broadening, and as the cell was saturated with water vapor, the density of the water vapor is known.

3. Line assignments

To help making line assignments, a new linelist for $H_2{}^{18}O$ was generated using the DVR3D program suite [18]. The program requires an external potential energy surface (PES) and a dipole moment surface (DMS) and uses variational techniques to calculate rotation–vibration energy levels of triatomic molecules. A good PES is essential for accurate prediction of energy levels. In this study, we have used the PES developed by Shirin et al. [19]. This PES was fitted to an extensive dataset of

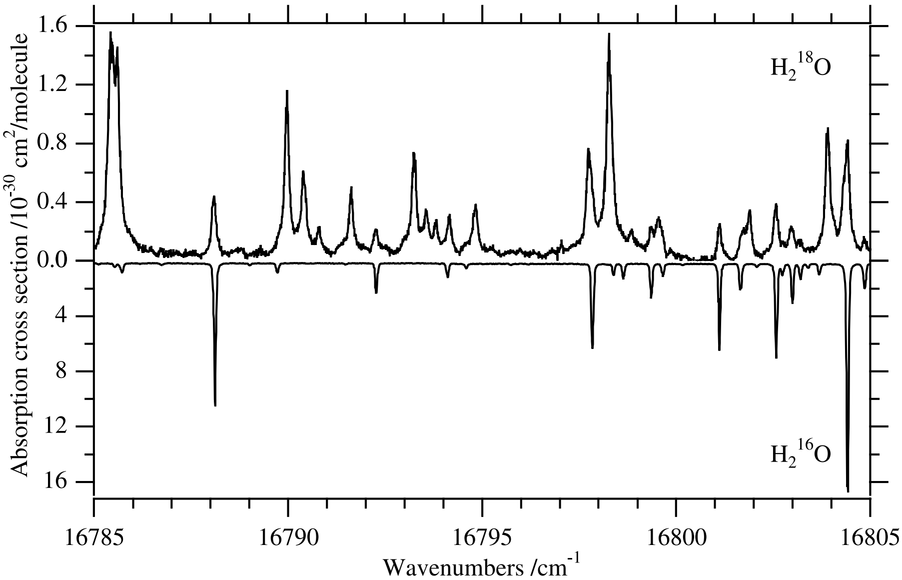

Fig. 1. A portion of the measured spectrum in $H_2{}^{18}O$ enriched water (top), compared with the natural water vapor spectrum previously measured by Naus et al. [14] (bottom). Lines only present in the top graph are $H_2{}^{18}O$ lines. The pressure at which the top graph was measured was 24 mbar, while the bottom graph was measured at about 16 mbar. The vertical axis in the top graph is a cross-section per molecule $H_2{}^{18}O$, the lines of $H_2{}^{16}O$ in this graph are scaled with the isotope ratio.

$H_2{}^{16}O$ energy levels including those generated from Naus et al.'s [14] cavity ring-down spectrum.

The following parameters were used to calculate the linelist. For vibrational states, Radau coordinates were selected. Thirty-four radial points based on a Morse oscillator-like functions [18] and 40 Gauss (associated) Legendre angular grid points were used to generate 2000 dimension final vibrational Hamiltonians. For rotationally excited states, the lowest 1000 vibrational functions were read for each value of k ($\approx K_a$) and final Hamiltonians of dimension $450 \times (J+1)$ were diagonalized up to $J = 10$. A temperature of 296 K (room temperature) was used for calculations of transitions. Fig. 2 compares the measured $H_2{}^{18}O$ absorption spectrum with our calculated linelist.

Initial assignments were made by comparing the experimental lines with the linelist, taking both frequency and intensity into consideration. Upper energy levels were then determined and all possible combinations of transitions were generated to search for further assignments by combination differences. Upper energy levels that were not confirmed by combination differences were

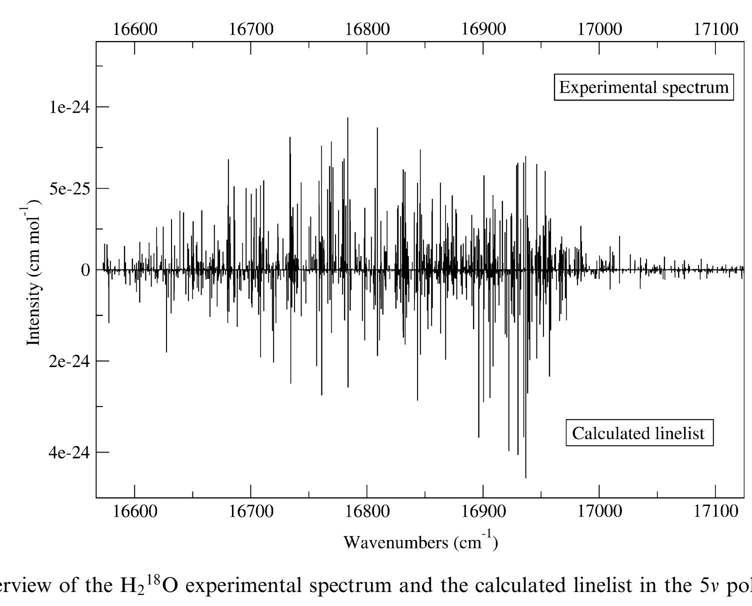

Fig. 2. Overview of the $H_2{}^{18}O$ experimental spectrum and the calculated linelist in the 5ν polyad region.

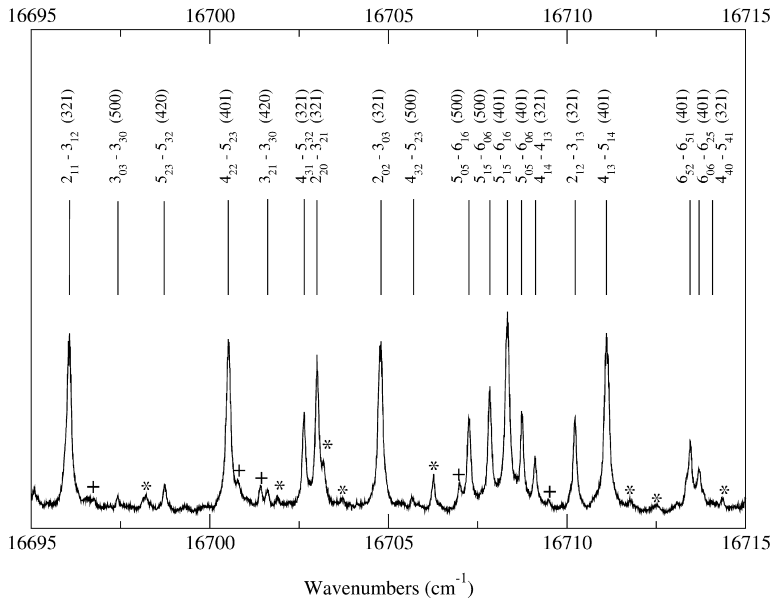

Fig. 3. Experimental spectrum in the 16 695–16 715 cm^{-1} range with the assignments. * indicates $H_2{}^{16}O$ lines and + indicates unassigned $H_2{}^{18}O$ lines.

re-considered and any necessary changes were made. Fig. 3 shows a part of spectrum with the assignments. The ratios of new energy levels of $H_2{}^{18}O$ to known $H_2{}^{16}O$ levels proved to be extremely helpful for checking the reliability of assignments, as it is known these ratios are approximately constant within a vibrational band [11].

We assigned 375 of the 596 $H_2{}^{18}O$ lines to 10 different upper vibrational levels. Table 1 shows the summary of the result. All transitions originate in the (000) ground vibrational level. Two new vibrational band origins were determined directly by transitions to their 0_{00} states: (321) at 16775.381 cm^{-1} and (401) at 16854.991 cm^{-1}. The band origin for (500) can be estimated at 16854.84 ± 0.02 cm^{-1} using the systematic error in our calculations. This procedure has been shown to work well in the past [20]. Table 2 shows the newly determined energy levels labeled with both normal and local mode notations. Obs – Calc shows the differences between an experimentally determined and the theoretically predicted energy level. All the assigned transitions and the energy levels can be found in the electronic archive.

Table 1
Summary of $H_2{}^{18}O$ energy levels determined in this study

Band	Origin (cm^{-1})	No. of levels	No. of trans.
(340) or $30^{+}4$	—	11	20
(241) or $30^{-}4$	—	7	12
(043) or $21^{-}4$	—	3	3
(142) or $21^{+}4$	—	12	19
(222) or $31^{+}2$	—	9	7
(420) or $40^{+}2$	—	29	39
(321) or $40^{-}2$	16775.381	42	83
(302) or $41^{+}0$	—	1	2
(500) or $50^{+}0$	16854.84	43	80
(401) or $50^{-}0$	16854.991	50	110
	Total	207	375

Bands are labeled using normal mode (left) and local mode (right) notations. No. of levels shows the number of newly determined energy levels. No. of trans. shows the number of transitions to the vibrational bands.

4. Discussion and conclusion

The reliability of the new linelist was first tested by analyzing the $H_2{}^{18}O$ spectrum in the 12 400–14 520 cm^{-1} range. In our previous study 747 of 927 lines were assigned using the linelist generated by Partridge and Schwenke [11]. With our new linelist, it was possible to make assignments to almost 900 lines. This test was particularly useful for checking the labeling of energy levels. Details will be given elsewhere [21].

Naus et al. assigned six of their transitions recorded using natural abundance water to $H_2{}^{18}O$. We find one of their lines was previously mis-assigned. The 16761.672 cm^{-1} line was assigned to 3_{13}–4_{14} 401–000 ($H_2{}^{18}O$) but the correct assignment is 5_{24}–5_{33} 142–000 ($H_2{}^{16}O$). The 3_{13}–4_{14} 401–000 ($H_2{}^{18}O$) line lies at 16761.004 cm^{-1}.

The absorption spectrum of $H_2{}^{18}O$ recorded using the cavity ring-down spectroscopy has been analyzed. Five hundred and ninety-six lines were identified as $H_2{}^{18}O$ and 375 of which are now assigned using the newly calculated linelist. The frequency range analyzed in this paper is the highest for $H_2{}^{18}O$ to date and the results should be useful for atmospheric and other studies.

Table 2
$H_2{}^{18}O$ energy levels in cm^{-1} for the (321), (500), and (401) vibrational states

J	K_a	K_c	(321) or 40^-2		Obs – Calc	(500) or 50^+0		Obs – Calc	(401) or 50^-0		Obs – Calc
0	0	0	16775.381	1	0.431				16854.991	1	−0.259
1	0	1	16797.751	2	0.436	16876.838	1	−0.152	16877.127	2	−0.165
1	1	1	16812.558	1	0.176	16887.674	2	−0.164	16887.956	1	−0.180
1	1	0	16818.257	1	0.132	16892.781	1	−0.145	16893.063	2	−0.173
2	0	2	16841.104	2	0.451	16919.565	1	−0.177	16919.869	1	−0.202
2	1	2	16851.770	2	0.410	16926.727	3	−0.166	16926.995	3	−0.166
2	1	1	16868.947	2	0.405	16941.961	1	−0.187	16942.284	3	−0.164
2	2	1	16912.252	1	−0.042	16975.261	1	−0.297	16975.532	1	−0.165
2	2	0	16913.804	2	0.281	16977.073	1	0.126	16976.948	3	−0.155
3	0	3	16903.088	2	0.423	16979.733	4	−0.070	16980.198	2	−0.117
3	1	3	16905.182	2	0.061	16984.457	2	−0.148	16984.835	2	−0.120
3	1	2	16943.465	2	0.392	17014.705	3	−0.145	17015.001	2	−0.140
3	2	2	16979.495	3	0.285	17041.940	2	−0.114	17041.964	2	−0.162
3	2	1	16986.445	2	0.249	17048.278	2	−0.104	17048.333	1	−0.171
3	3	1	17115.166	2	−0.054	17059.953	2	−0.328	17061.423	4	0.071
3	3	0	17115.365	2	−0.085	17060.270	3	−0.258	17061.659	1	0.060
4	0	4	16979.033	2	0.384	17058.157	1	−0.181	17058.363	1	−0.147
4	1	4	16983.912	1	−0.020	17060.221	1	−0.196	17060.411	2	−0.163
4	1	3	17040.529	3	0.359	17109.231	2	−0.165	17109.490	3	−0.159
4	2	3	17067.391	1	0.284	17129.480	2	−0.060	17129.345	2	−0.145
4	2	2	17084.209	3	0.275	17145.664	2	−0.104	17145.670	4	−0.131
4	3	2	17206.628	1	−0.292	17150.823	2	−0.125	17151.466	3	−0.026
4	3	1	17208.361	3	−0.065	17152.405	2	0.014	17152.249	3	−0.057
4	4	1				17250.003	1	−0.291	17250.636	1	−0.259
4	4	0	17318.857	2	0.217	17250.447	2	0.112	17250.811	1	−0.060
5	0	5	17076.303	1	0.033	17152.600	3	−0.154	17153.584	3	−0.148
5	1	5	17077.137	1	0.403	17152.692	2	−0.153	17153.671	3	−0.150
5	1	4	17157.904	3	0.310	17223.347	1	−0.232	17223.609	3	−0.146
5	2	4	17175.241	3	0.252	17237.120	1	−0.074	17236.784	4	−0.122
5	2	3	17207.731	4	0.259	17268.684	2	−0.044	17268.425	2	−0.110
5	3	3	17321.491	4	0.146	17263.668	3	−0.052	17264.399	4	−0.077
5	3	2	17326.788	2	−0.012	17269.334	3	−0.062	17268.533	2	−0.401
5	4	2	17435.397	1	0.287	17363.369	1	−0.082	17363.554	2	−0.343
5	4	1	17435.068	2	−0.256	17363.475	3	−0.322	17363.609	2	0.065
5	5	1	17496.634	1	−0.217	17456.692	2	0.020	17456.947	2	−0.004
5	5	0				17456.703	2	0.025	17456.722	1	−0.236
6	0	6							17264.145	2	−0.133
6	1	6				17263.546	2	−0.142	17264.166	2	−0.131
6	1	5	17293.138	3	0.238	17355.452	1	−0.087	17355.477	3	−0.102
6	2	5				17364.686	1	0.047	17363.699	2	0.200
6	2	4							17411.992	3	−0.122
6	3	4	17458.118	3	−0.012	17399.119	2	0.475	17399.527	5	−0.077
6	3	3	17471.645	3	−0.019	17411.699	1	0.388	17409.519	1	−0.152
6	4	3				17499.669	1	0.255	17499.726	2	−0.341
6	4	2	17575.652	1	−0.385				17501.234	2	−0.374
6	5	2							17593.567	2	0.047
6	5	1							17593.561	2	−0.023
6	6	0							17726.192	1	−0.215
7	1	7							17391.441	2	−0.141
7	1	6				17503.917	2	0.237			
7	2	6	17447.102	1	0.159						
7	3	5	17616.343	2	0.097						
7	3	4	17642.801	2		17575.265	3	−0.377			
8	0	8							17535.562	2	−0.128

Also given are the number of transitions assigned to each level and the differences Obs – Calc, experimentally determined levels compared to our theoretical predictions.

Acknowledgments

This work is supported by the Space Research Organisation Netherlands (SRON) and by the European Community—Access to Research Infrastructures action of the Improving Human Potential Program, Contract No. HPRI-CT-1999-00064.

References

[1] R. Lang, A.N. Maurellis, W.J. van der Zande, I. Aben, J. Landgraf, W. Ubachs, J. Geophys. Res. 107 (D16) (2002) 4300.

[2] R.A. Toth, J. Mol. Spectrosc. 190 (1998) 379–396.

[3] R.A. Toth, J. Opt. Soc. Am. B 9 (1992) 462–482.

[4] R.A. Toth, J. Opt. Soc. Am. B 10 (1993) 1526–1544.

[5] R.A. Toth, J. Mol. Spectrosc. 166 (1994) 184–203.

[6] R.A. Toth, Appl. Opt. 33 (1994) 4868–4879.

[7] J.P. Chevillard, J.-Y. Mandin, J.-M. Flaud, C. Camy-Peyret, Can. J. Phys. 63 (1985) 1112–1127.

[8] J.P. Chevillard, J.-Y. Mandin, J.-M. Flaud, C. Camy-Peyret, Can. J. Phys. 64 (1986) 746–761.

[9] J.P. Chevillard, J.-Y. Mandin, J.-M. Flaud, C. Camy-Peyret, Can. J. Phys. 65 (1987) 777–789.

[10] A. Bykov, O. Naumenko, T. Petrova, A. Scherbakov, L. Sinitsa, J.Y. Mandin, C. Camy-Peyret, J.-M. Flaud, J. Mol. Spectrosc. 172 (1995) 243–253.

[11] M. Tanaka, J.W. Brault, J. Tennyson, J. Mol. Spectrosc. 216 (2002) 77–80.

[12] C. Camy-Peyret, J.-M. Flaud, J.-Y. Mandin, A. Bykov, O. Naumenko, L. Sinista, B. Voronin, J. Quant. Spectrosc. Radiat. Transfer 61 (1998) 795–812.

[13] L.S. Rothman, A. Barbe, D.C. Benner, L.R. Brown, C. Camy-Peyret, M.R. Carleer, K. Chance, C. Clerbaux, V. Dana, V.M. Devi, A. Fayt, J.-M. Flaud, R.R. Gamache, A. Goldman, D. Jacquemart, K.W. Jucks, W.J. Lafferty, J.Y. Mandin, S.T. Massie, V. Nemtchinov, D.A. Newnham, A. Perrin, C.P. Rinsland, J. Schroeder, K.M. Smith, M.A.H. Smith, K. Tang, R.A. Toth, J.V. Auwera, P. Varanasi, K. Yoshino, J. Quant. Spectrosc. Radiat. Transfer 82 (2003) 5–44.

[14] H. Naus, W. Ubachs, P.F. Levelt, O.L. Polyansky, N.F. Zobov, J. Tennyson, J. Mol. Spectrosc. 205 (2001) 117–121.

[15] H. Naus, I.H.M. van Stokkum, W. Hogervorst, W. Ubachs, Appl. Opt. 40 (2001) 4416–4426.

[16] S. Gerstenkorn, P. Luc, Atlas du Spectroscopie d'Absorption de la Mol-cule de l'Iode Entre 14 800–20 000 cm^{-1}, Presses du CNRS, Paris, 1978.

[17] J.T. Hodges, J.P. Looney, R.D. van Zee, Appl. Opt. 35 (1996) 4112–4116.

[18] J. Tennyson, M.A. Kostin, P. Barletta, G.J. Harris, J. Ramanlal, O.L. Polyansky, N.F. Zobov, Comp. Phys. Commun. (in press).

[19] S.V. Shirin, O.L. Polyansky, N.F. Zobov, P. Barletta, J. Tennyson, J. Chem. Phys. 118 (2003) 2124–2129.

[20] N.F. Zobov, D. Belmiloud, O.L. Polyansky, J. Tennyson, S.V. Shirin, M. Carleer, A. Jenouvrier, A.-C. Vandaele, P.F. Bernath, M.F. Merienne, R. Colin, J. Chem. Phys. 113 (2000) 1546–1552.

[21] M. Tanaka, J.W. Brault, J. Tennyson, O. Naumenko, to be submitted.